

# PROCEEDINGS OF SPIE

[SPIDigitalLibrary.org/conference-proceedings-of-spie](https://SPIDigitalLibrary.org/conference-proceedings-of-spie)

## Broadband microwave imaging spectroscopy with a solar-dedicated array

Tim S. Bastian, Dale E. Gary, S. M. White, Gordon J. Hurford

Tim S. Bastian, Dale E. Gary, S. M. White, Gordon J. Hurford, "Broadband microwave imaging spectroscopy with a solar-dedicated array," Proc. SPIE 3357, Advanced Technology MMW, Radio, and Terahertz Telescopes, (31 July 1998); doi: 10.1117/12.317414

**SPIE.**

Event: Astronomical Telescopes and Instrumentation, 1998, Kona, HI, United States

# Broad-band microwave imaging spectroscopy with a solar-dedicated array

T.S. Bastian<sup>a</sup>, D.E. Gary<sup>b</sup>, S.M. White<sup>c</sup> and G.J. Hurford<sup>d</sup>

<sup>a</sup>National Radio Astronomy Observatory\*, P.O. Box 'O', Socorro, NM 87801

<sup>b</sup>Physics Department, New Jersey Institute of Technology, Newark, NJ 07102

<sup>c</sup>Department of Astronomy, University of Maryland, College Park, MD 20742

<sup>d</sup>Solar Astronomy 264-33, Caltech, Pasadena, CA 91125

## ABSTRACT

For many years, ground-based radio observations of the Sun have proceeded in two directions: i) high resolution imaging at a few discrete wavelengths; ii) spectroscopy with limited or no spatial resolution at centimeter, decimeter, and meter wavelengths. Full exploitation of the radio spectrum to measure coronal magnetic fields in both quiescent active regions and flares, to probe the thermal structure of the solar atmosphere, and to study energy release and particle energization in transient events, requires a solar-dedicated, frequency-agile solar radiotelescope, capable of high-time, -spatial, and -spectral resolution imaging spectroscopy. In this paper we summarize the science program and instrument requirements for such a telescope, and present a strawman interferometric array composed of many (> 40), small (2 m) antenna elements, each equipped with a frequency-agile receiver operating over the range 1–26.5 GHz.

**Keywords:** Radio interferometry, spectroscopy, optical fiber, correlator

## 1. INTRODUCTION

Solar observations at radio wavelengths provide a unique perspective on virtually all phenomena in the solar atmosphere. Historically, exploration of radio emission from the Sun has proceeded along two essentially orthogonal lines. Imaging observations have been performed at discrete frequencies with interferometric arrays. In the past two decades, in the meter wavelength range, these have included the Culgoora Radioheliograph, the Clark Lake Radio Observatory, and the Nançay Radioheliograph. At centimeter wavelengths, the imaging instruments have been the Very Large Array (VLA) and the Westerbork Synthesis Radio Telescope (both non-solar-dedicated), and the Nobeyama Radioheliograph. A second line of inquiry has involved spatially unresolved spectroscopy using fixed-frequency polarimeters or spectrographs. Examples include the polarimeters at Toyokawa, Nobeyama, and Berne, the PHOENIX spectral polarimeter at Bleien, the survey sweep spectrographs at Culgoora and Tretsdorf, and the USAF Solar Radio Burst Locators (SRBL).

In order to fully exploit the diagnostic potential of radio emission from the Sun, it is essential to perform both imaging and spectroscopy simultaneously. There is only one instrument that has combined two-dimensional imaging and spectroscopic capabilities: the Owens Valley Radio Observatory (OVRO) solar array, a solar-dedicated five-element array that is frequency agile between 1–18 GHz.<sup>1</sup> The OVRO solar array has demonstrated the utility of imaging spectroscopy and has served to motivate the case for a next generation instrument: a Frequency Agile Solar Radio Telescope (FASR). A consensus exists among the international solar radio community, as expressed at an NSF/NASA supported Solar Radio Telescope Workshop held in San Juan Capistrano in 1995, that it is possible, highly desirable, and timely, to construct an advanced, solar-dedicated radiotelescope designed to perform broad-band imaging spectroscopy. Here we briefly describe the science program and science requirements of the instrument, and present a strawman instrument design for the FASR.

\* The National Radio Astronomy Observatory is a facility of the national Science Foundation operated under a cooperative agreement by Associated universities, Inc.

Correspondence: TSB – E-mail: tbastian@nrao.edu; Tel: (505) 835-7259, DEG – E-mail: dgary@njit.edu; Tel: (973) 642-7878

## 2. SCIENCE OBJECTIVES

The radio spectrum at decimeter and centimeter wavelengths is rich in diagnostic potential. At least four distinct radio emission mechanisms are relevant at these wavelengths: (i) *plasma emission*, which results from the nonlinear excitation of plasma waves and their subsequent conversion to electromagnetic waves, typically seen at decimeter and longer wavelengths during flares; (ii) *thermal bremsstrahlung*, resulting from collisions between electrons and ions, and occurring throughout the solar atmosphere; (iii) *thermal gyroresonance emission*, which results from the acceleration of thermal electrons by the Lorentz force as they spiral around in strong magnetic fields, and is therefore associated with sunspots and solar active regions; and (iv) *gyrosynchrotron emission*, which is produced by thermal or nonthermal populations of energetic electrons (10s of keV to several MeV) spiraling about magnetic fields, typically seen during energetic phenomena such as flares. Each of these emission mechanisms is sufficiently well understood that it may be exploited to diagnose physical conditions on the Sun.

The major advance offered by the FASR is time-resolved, broad-band imaging spectroscopy – it will produce high resolution images at closely spaced frequencies over a broad frequency range, or equivalently, brightness temperature spectra at every point within the field of view of the instrument. For the first time, it will enable users to fully exploit the diagnostic potential of radio emission at decimeter and centimeter wavelengths for phenomena varying on the short time scales characteristic of the Sun. The variability and unpredictability of the solar phenomena, as well as the distinct imaging and spectroscopic requirements, clearly require a solar-dedicated instrument. As such, the FASR will be widely used by the general solar community. FASR will also be of great value for space weather research and forecasting of geophysical effects, since the nature of radio data processing makes it easy to monitor phenomena in real time and broadcast alerts automatically. It will also offer important proxies for irradiance and spectral inputs to models extensively employed by the ionospheric and aeronomy communities.

The FASR is required to perform broad-band imaging spectroscopy over a core frequency range of 1–26.5 GHz. Moreover, it is designed to do so on the relevant spatial, spectral, and temporal scales. These are demanding requirements designed to address a broad program of science, including particle heating and acceleration in transient energetic events (flares and coronal mass ejections), mechanisms of energy storage and release, mechanisms of energy transport, the structure of the solar atmosphere, and the structure and evolution of coronal magnetic fields. We cannot review the full program of science here. However, before discussing the instrument requirements, we highlight several key elements of the science program.

### 2.1. Coronal magnetography

Quantitative knowledge of coronal magnetic fields is crucial to virtually all solar physics above the photosphere, including the structure and evolution of active regions, flares, filaments, and coronal mass ejections (CMEs). For this reason, considerable resources are devoted to the measurement of magnetic fields in the photosphere and low-chromosphere, where optical and infrared techniques may be employed. Soft x-ray imaging provides striking indications of the morphology of coronal fields (e.g., Ref. 2), but no information on their strength. The coronal magnetic field must be inferred by extrapolating the observed surface magnetic field distribution into the upper chromosphere and corona under the assumption that it is potential or force-free. An example of such a force-free magnetic field extrapolation is shown in Figure 1. These extrapolations are difficult, depend sensitively on measurements at the photospheric level, and rely on assumptions that need to be more thoroughly tested.

Radio observations provide the only means by which coronal magnetic field strengths  $\gtrsim 100$  G can be measured above the chromosphere. The longitudinal field can be obtained rather directly at the base of the corona by exploiting the break in the spectrum of thermal gyroresonance emission where the electron temperature drops to sub-coronal values. However, the FASR will, in addition, enable us to constrain the vector magnetic field and its evolution in active regions. Figure 1 shows how gyroresonance emission at different frequencies arises on nested surfaces of constant magnetic field which differ for the two polarizations. The dense spectral sampling provided by FASR provides complete sampling of the coronal volume over active regions. When coupled with extrapolation techniques FASR observations provide the means of performing three-dimensional coronal magnetography where the magnetic field strength exceeds  $\approx 100$  G. Such measurements of the evolving magnetic field in and above active regions will offer much needed insight into the storage and release of magnetic energy.

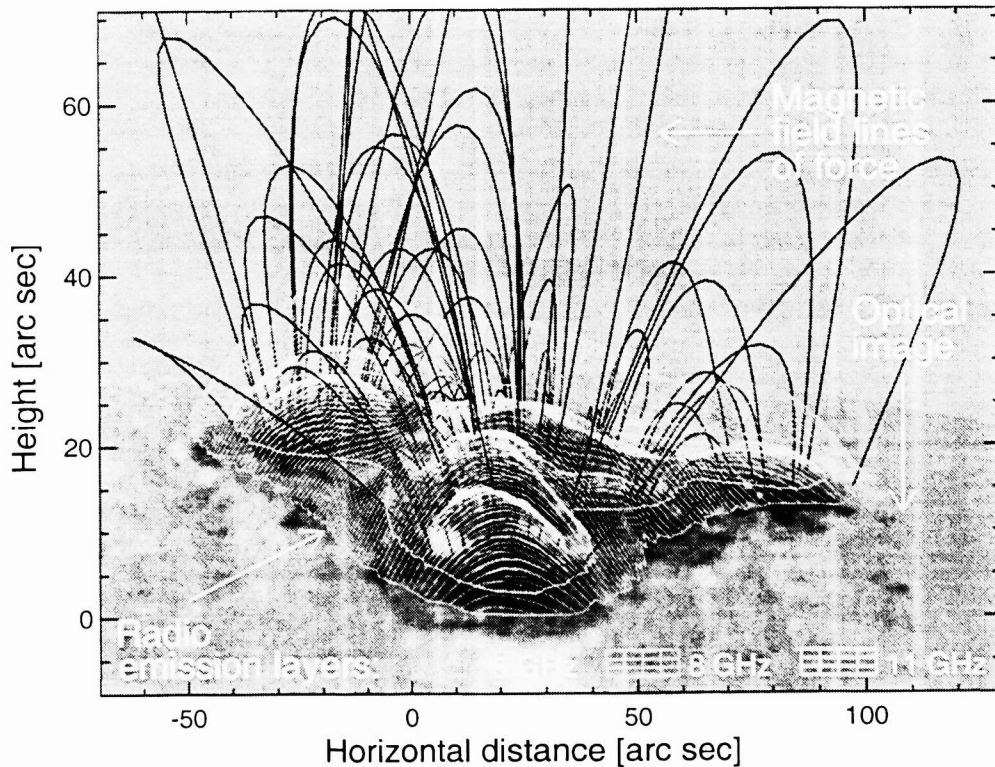


**Figure 1.** A perspective view of a complex sunspot group (7 May 1991) in optical continuum is shown with field lines extrapolated into the corona using a nonlinear force-free extrapolation by Z. Mikić. The three surfaces are the calculated gyroresonant surfaces in the corona that will dominate the radio opacity at each of three radio frequencies: 5 GHz ( $B = 600$  G), 8 GHz ( $B = 950$  G) and 11 GHz ( $B = 1300$  G). (Produced by Jeongwoo Lee/NJIT.)

## 2.2. Thermal structure of the solar atmosphere

In weak field regions where thermal gyroresonance emission is largely absent, radio emission remains sensitive to thermal structure through thermal bremsstrahlung emission. An important feature of radio observations of thermal plasma is that they act as a true thermometer, the radio emission being directly proportional to the electron temperature. By contrast, the conversion of observations of atomic lines into temperature information is model-dependent. By varying the observing frequency  $\nu$  from 1–26.5 GHz, one samples the thermal state of optically thick plasma from the mid-chromosphere to the low-corona. It has become increasingly apparent that the prevailing semi-empirical chromospheric models, largely based on non-LTE UV/EUV line and IR/submm/mm continuum observations and computed under the assumption of hydrostatic equilibrium, are incorrect: they are not consistent with either the detection of CO in the atmosphere, which requires the presence of cool (3800 K) material,<sup>3</sup> or with accurate broadband microwave (spatially unresolved) spectroscopy of the quiet Sun.<sup>4</sup> The FASR design will allow us to sample the thermal structure of the chromosphere down to the height where  $T_e \sim 8000$  K with a frequency-dependent angular resolution of 2.5–6". FASR observations will provide a comprehensive specification of the thermal structure of the chromosphere—in coronal holes, quiet regions, enhanced network, plages—as an input for modern models of the inhomogeneous and dynamic chromosphere.

## 2.3. Flares and coronal mass ejections

The FASR will, for the first time, allow full exploitation of microwave/decimetric emission for flare studies. The possibilities are numerous and exciting:

*Magnetic field in the flaring volume:* Microwave emission in flares is due to incoherent gyrosynchrotron emission from electrons with energies of several 10s of keV to several MeV. The peak spectral frequency  $\nu_{pk}$  at a given location depends sensitively on the local magnetic field strength and the angle between the wave normal and the magnetic field vector. Joint observations of  $\nu_{pk}$  and the source polarization will allow the magnetic field strength and orientation to be constrained for the flaring source as a function of time. No other technique is available for this purpose.

*Electron acceleration and transport:* The microwave spectrum is a powerful diagnostic of the details of the distribution of the emitting electrons. The optically thin part of the spectrum is sensitive to high energy cutoffs in the spectrum and to anisotropies in the distribution function. The relative timing of temporal features at different frequencies and locations offers an additional diagnostic of acceleration and transport.

*Location and properties of the energy release site:* Multitudes of type III and reverse drift type III bursts—resulting from bidirectional electron beams—accompany the impulsive phase of many flares.<sup>5</sup> While spectroscopic observations of classical and reverse-drift type IIIs during flares have been performed, few have been imaged. The FASR will identify the location of these bursts, presumably intimately related to the primary energy release, and trace their trajectories both upward and downward in the flaring volume.

*Chromospheric ablation:* In addition to diagnosing the magnetic field and the details of the energetic electron population, radio observations offer a means of probing the density and evolution (due, for example, to chromospheric ablation) of the ambient plasma by means of Razin suppression, the specifics of which depend on the density of the ambient plasma and the local magnetic field strength.

*CME detection:* Coronal mass ejections have become the main focus of studies of space weather and the near-Earth space environment. Ref. 6 has shown that, with support at frequencies  $< 1$  GHz, the FASR may also be used for CME detection. The advantages of CME detection at radio wavelengths are: i) there is no occulting disk, so earth-directed CMEs will be detected; ii) CMEs will be detected in their nascent stages of development and can be directly associated with structures such as filament channel arcades; iii) unlike SXR and white-light observations, observations at radio wavelengths are sensitive to both thermal free-free emission from CMEs and possible nonthermal constituents. Owing to its frequency agility the FASR could provide a comprehensive observational picture of CMEs and associated phenomena over a wide frequency range.

## 2.4. Synoptic measurements

The solar 10.7 cm flux has been used for many years as a proxy indicator of solar activity due to its close correlation with other diagnostics such as sunspot number and area, the emission in Ly $\beta$ , Mg II, and EUV fluxes, and the total solar irradiance. The 10.7 cm flux remains the solar measurement in highest demand amongst the space weather community. However, Ref. 7 has shown that multi-radio-frequency measurements can be combined to yield superior proxies for both sunspots and irradiance. FASR will provide well-calibrated multifrequency observations suitable for exploiting such diagnostics, but one can envision many other synoptic studies with an instrument like the FASR. For example, with high-resolution, spatially resolved maps at each frequency, synoptic studies of the gyroresonance component of the radio emission and hence, the coronal magnetic field, could be performed. Such observations require accurate and stable calibration over long periods of time. FASR will achieve this by calibrating against cosmic standards.

## 3. INSTRUMENT REQUIREMENTS

The primary goal is to design and construct an instrument that fully exploits solar microwave emission as a diagnostic of physical processes on the Sun. To this end, a number of instrumental requirements have been identified:

1. *Imaging:* The sources of radio emission on the Sun must be imaged with high dynamic range, fidelity, and angular resolution, with good sensitivity to both compact and extended sources of emission. A dynamic range of order 1000:1 and angular resolution of  $\approx 1''$  at a frequency of 20 GHz are considered reasonable goals.
2. *Broad-Band spectroscopy:* The brightness temperature spectrum as a function of position is the required observable. Spectral coverage over a core frequency range of 1–26.5 GHz is therefore required. Matched resolution at selected frequencies is highly desirable.

3. *Polarimetry*: Observations in both the right- and left-hand senses of circular polarization are needed to form the Stokes **I** and **V** polarization parameters.
4. *High time resolution*: Brightness temperature spectra must be acquired at a rate sufficient to resolve the time scale on which phenomena of interest evolve. The most demanding requirement is imposed by the impulsive phase of flares, which will require a time resolution of  $< 1$  sec.
5. *Large field of view*: In the interest of maximizing observing efficiency and in matching the capabilities of existing full disk spectrographs and imagers at other wavelengths, a full disk imaging capability is desired at most frequencies.
6. *Good absolute positional accuracy*: Instruments in most wavelength bands now possess an angular resolution ranging from less than 1 arcsec to several arcsec. Quantitative cross-comparisons between various wavelength regimes will require absolute source positions to a similar accuracy.
7. *Upgradability*: The instrument should be designed with future upgrades in mind. Examples include support of very high-time- and high-frequency-resolution observations of decimetric phenomena and the extension of frequency coverage to lower and higher frequencies.
8. *Easy access by the solar community*: The instrument should not place the burden of data reduction on the user. Most reductions should be performed on-site and a wide variety of data products should be made available for immediate and open use by the community at large.

#### 4. A STRAWMAN DESIGN

High-angular-resolution imaging at radio wavelengths requires an instrument that employs Fourier synthesis imaging using an interferometric array of antennas. We therefore take as our starting point the assumption that the FASR will be an array of antennas. We begin with a consideration of the optimum array configuration and then consider the important issues of antennas, analog signal processing and transmission, digitization, and correlation.

##### 4.1. Antenna configuration

A Fourier synthesis telescope measures the Fourier transform of the radio brightness distribution, the so-called *visibility function*. The sampling of the visibility function is determined by the cross-correlation function of the antenna locations in the array. The point spread function (PSF) of the array is the inverse Fourier transform of the sampling function. The criteria by which antenna configurations are assessed depend on the imaging problem at hand. For a two-dimensional array of finite extent, uniform sampling in the Fourier, or  $uv$ , plane yields both the highest angular resolution and the best signal to noise ratio.<sup>8</sup> Hence, a commonly employed criterion for assessing general purpose astronomical array configurations has been uniformity of sampling in the  $uv$  plane. However, additional criteria often come into play. In the case of the VLA,<sup>9</sup> reconfigurability, scalability, and a practical means of accomplishing both led designers to choose a “Y” configuration of three linear arrays of nine antennas each. The distance of each antenna from the center of the array along each arm is given by a power law,  $d \propto n^\alpha$ , where  $n = 1, 2, 3, \dots, 9$ , yielding a nonuniform, centrally-condensed sampling function.

The FASR is a special-purpose instrument. It will observe the Sun at a large number of frequencies between 1–26.5 GHz with a fixed array configuration. The signal to noise ratio is not an over-riding concern for a strong source like the Sun. Hence, uniform sampling is not a determining criterion. Indeed, it is far more important to consider the visibility function of the Sun and to ensure that the sampling function adequately samples the relevant spatial scales. The visibility function of the Sun is, to first order, the Hankel transform of a uniform disk:  $J_1(\pi q \theta_D)/(\pi q \theta_D)$ , where  $J_1$  is a first order Bessel function,  $q = \sqrt{u^2 + v^2}$  is the spatial frequency, and  $\theta_D$  is the angular diameter of the solar disk. Structure of interest is superposed on this dominant functional form. Except during times of strong activity, the transform of the disk dominates the visibility function at all frequencies for  $q \lesssim 1000\lambda$ , or baselines  $b \lesssim 300$  m at 1 GHz and  $b \lesssim 15$  m at 20 GHz.

The science requirements emphasize both high resolution studies (1'' at 20 GHz) and studies of large scale phenomena comparable to the scale of the solar disk (e.g., filament channels, prominence eruptions). It is therefore necessary to adequately sample the solar visibility function over three orders of magnitude in spatial frequency! By

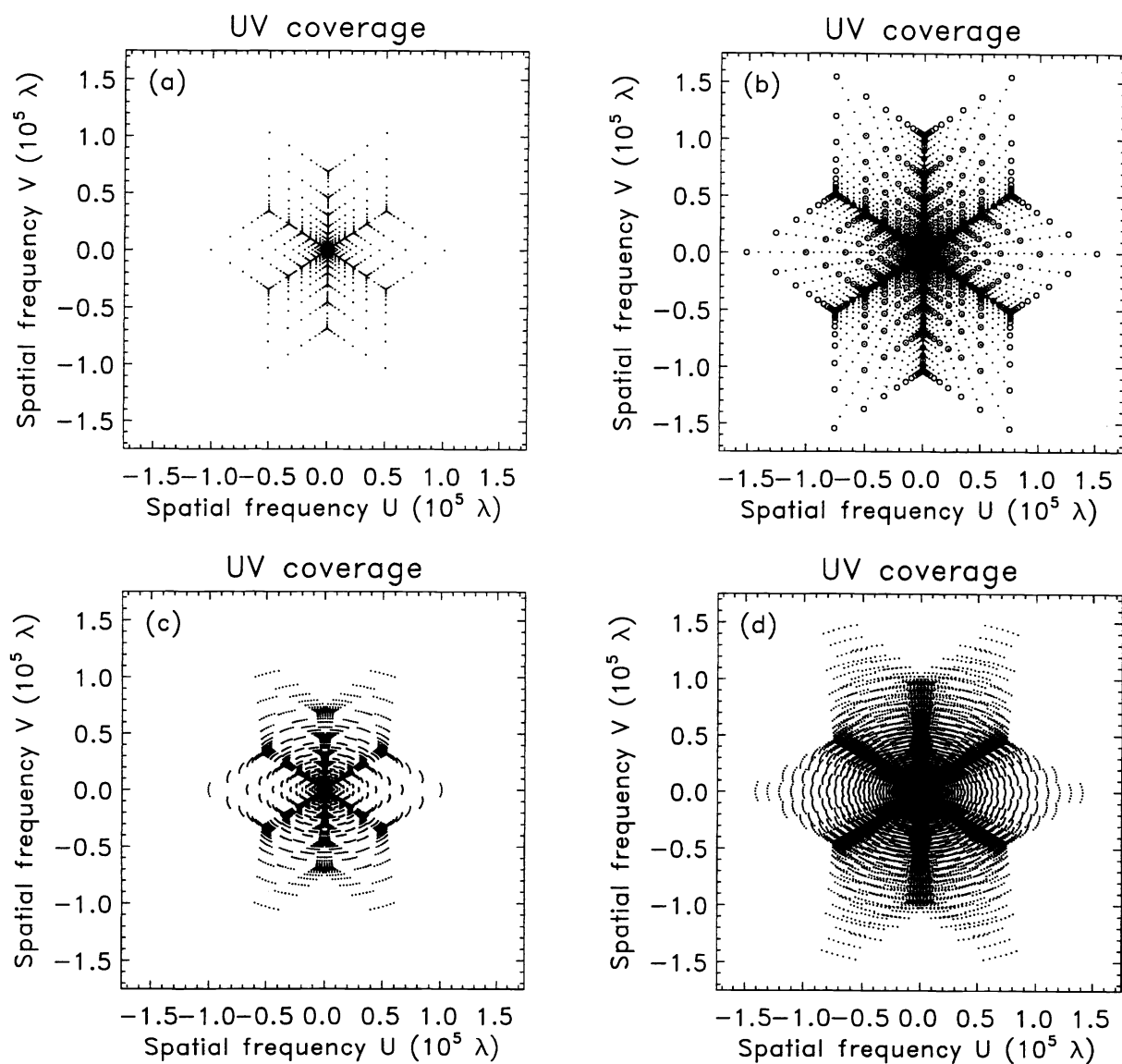


**Figure 2.** An example of the  $uv$  coverage resulting from a 43-element, self-similar array, with 14 antennas along each of three arms with a shared element in the middle. The array is assumed to be at a latitude of  $35^\circ$ . The Sun is assumed to be on the meridian, at a declination of  $20^\circ$ . a) The snapshot  $uv$  coverage at a frequency of 10 GHz; b) The snapshot coverage for six frequencies: 10, 11, 12, 13, 14 GHz (points) and 15 GHz (open circles). Note that the  $uv$  coverage at 10 and 15 GHz is identical except on the outermost and innermost  $uv$  points; c) The  $uv$  coverage obtained in 20 min at a frequency of 10 GHz; d) The  $uv$  coverage obtained in 20 min at frequencies of 10, 11, 12, 13, and 14 GHz.

comparison, the ratio of the maximum to minimum spatial frequencies sampled by a given configuration of the VLA is 40. Furthermore, the requirement of high time resolution imaging means the instantaneous sampling of the  $uv$  plane by the FASR must be excellent. Finally, matched PSFs are highly desirable at selected frequencies. How can these requirements be met with a fixed array composed of a relatively small number of antennas?

We propose to meet these requirements with a simple array configuration which, like the VLA or the Nobeyama Radioheliograph, is composed of three (or more) linear arms. Unlike these arrays, we choose antenna spacings according to an exponential law,  $s = c a^n$ ,  $n = 1, 2, 3, \dots, N$ , where  $N$  is the number of antennas on each arm. The distance of the  $n$ th antenna from the center of the array is then  $d = c \sum_{i=1}^n a^i$ . The spatial frequency sampled by an antenna baseline  $\mathbf{b}$  is  $\mathbf{b}(\nu/c)$ ; the sampling function therefore scales with frequency. Sampling in the radial direction in the  $uv$  plane can therefore be improved by sampling over a limited spectral bandwidth, a technique referred to as “frequency synthesis”.<sup>10,11</sup> The proposed configuration lends itself naturally to frequency synthesis: for example, if  $a = 1.5$ , sampling over a bandwidth of 50% yields complete sampling in the radial direction. Furthermore, for all frequency pairs with a ratio of  $\nu_1/\nu_2 = 1.5^m$ ,  $m$  an integer, the  $uv$  coverage is identical for the two frequencies over most of the  $uv$  plane, thereby yielding identical PSFs (Figure 2a,b). The array is “self-similar” in this sense. While frequency synthesis can fill in the  $uv$  coverage in the radial direction, no such technique is available for further improving the instantaneous azimuthal coverage. However, the kinds of imaging problems that require high time resolution, and therefore rely on the instantaneous  $uv$  coverage, do not generally require sampling on the largest angular scales. Hence, while the sampling is sparser in the azimuthal coordinate, it is still sufficient for most compact, dynamic phenomena. For experiments that require mapping on all angular scales, earth rotation aperture synthesis must be used to fill in the azimuthal sampling. For the sample configuration shown in Figure 2,  $\approx 20$  min is required for complete sampling in the azimuthal direction (Figure 2c,d).

In summary, a fixed array with a self-similar (exponential) distribution of antenna spacings along linear arms offers several appealing characteristics: 1) it lends itself naturally to frequency synthesis techniques; 2) it contains embedded scaled array configurations; 3) it samples the solar visibility function in a more optimum way than does an array designed to produce uniform sampling of the  $uv$  plane; 4) at a more practical level, the linear arms of the array allow shorter runs of cables to the antennas and easier access for maintenance.

## 4.2. Antennas and feeds

The requirement of full disk imaging at most frequencies implies the use of small antenna elements. For concreteness, let us suppose that we observe the full disk of the Sun to a frequency of 15 GHz. This implies an antenna size of 2 m. On the other hand, the need for good absolute calibration implies a need for astronomical calibration (see §4.6); i.e., referencing solar visibility measurements to sidereal sources with accurately known positions and fluxes. This requires sufficient sensitivity to sidereal sources which, in turn, implies a need for large, sensitive antennas. Hence, in addition to many small antennas, the strawman design calls for one or more large antennas. These would likely be sited at the outermost antenna stations for increased sensitivity on the longest baselines.

The front ends (feeds, low-noise amplifiers (LNAs), and mixers) must be very broad-band. The SRBL telescope design employs a logarithmic spiral feed sensitive to the 1–18 GHz range while the OVRO solar array employs both spiral feeds and log-periodic linear feeds in a hybrid scheme that maximizes sensitivity while allowing circular polarization measurements to be made. These instruments both employ 0.1–18 GHz FET preamplifiers with a room-temperature noise figure of 2.3 dB, and 1–18 GHz mixer/preamps.

For the FASR, log-periodic crossed-dipole feeds will likely be employed. The feeds, LNAs, and mixer/preamps will need 1–26.5 GHz bandwidths or else switchable, separate signal paths for 1–18 GHz and 18–26.5 GHz can be used.

## 4.3. Analog signal processing

Conventionally, the input radio frequency (RF) at each antenna is converted to an intermediate frequency (IF) by mixing it with a local oscillator (LO) signal slaved to a master oscillator. These operations take place at the antenna and the IF is then transmitted to a central location for further processing. Within such a scheme, the requirement of high time resolution might appear to impose severe demands on the system. However, the entire spectrum need not be sampled instantaneously, and the frequency resolution and rate at which spectra are acquired depends on the phenomenon of interest. The high flux levels from the Sun allow fast sampling with good signal to noise. Thus



one option is to assume that 500 MHz wide sections of the total bandwidth will be sampled sequentially; i.e., that frequency multiplexing will be performed.

To cover the broad frequency range (1-26.5 GHz), the FASR will require  $\sim 50$  separate tunings of the 500 MHz bandwidth IF. The science requirement calls for the entire spectrum to be covered in 1 s or less. Thus, the required tuning, phase lock, and data acquisition must occur in  $\lesssim 20$  msec, for each frequency sampled. The general scheme for accomplishing this will be similar to the system currently employed at the OVRO Solar Array, whose operation is outlined as follows:

The receivers of the OVRO Solar Array employ YIG-tuned LOs, which can be tuned continuously over their range by supplying a coarse tuning current and then fine-tuning via an FM port (a frequency-modulation port, so-named because it can be used to frequency-modulate the LO output). The full 1-18 GHz range at OVRO is covered by three LOs, whose individual ranges are 1-2 GHz, 2-8 GHz, and 8-18 GHz. A coarse tuning current is selected digitally by the controlling computer and supplied to the relevant oscillator. The output of the oscillator is then mixed with harmonics of a 200 MHz reference signal from a comb generator. When the tuning current corresponds sufficiently closely to a harmonic of 200 MHz, the output of the mixer is compared with a second, 1 MHz reference signal to form an error signal that is used to phase lock the system via corrections to the oscillator's FM port (fine tuning). Phase lock for frequencies within the same oscillator can be acquired typically within 10 ms. The current sample time used at OVRO is 20 ms, although this will shortly be reduced to 10 ms with the introduction of a faster control computer. When switching frequencies as rapidly as possible phase lock is acquired during one sample and data are taken during the following sample for a duty-cycle of 50%. Thus, at the 10 ms per sample rate, the most rapid effective data rate will be one sample per 20 ms.

Only minor modifications to this scheme would be required for use with the FASR. A fourth oscillator would be needed for the 18-26.5 GHz range and the 200 MHz reference signal must be replaced with a 500 MHz reference since the IF bandwidth will be 500 MHz. At least two IF channels, one for each sense of circular polarization, would be required. Additional IF pairs may be desirable. The 50% duty-cycle in data acquisition can be avoided by using two sets of LOs and phase lock systems in each receiver. This redundancy would allow data to be taken at one frequency while phase lock is being acquired for the next frequency.

A more radical alternative to that outlined above is to simply transmit the entire RF segment of 1-26.5 GHz from the antennas to a central location. This approach would obviate the need for LOs, mixers, and phase-lock loops in each antenna and the distribution of reference signals to all antennas. It would, however, require a single amplifier, switchable attenuators, and possibly an injected broad-band calibration signal. The advantages of this approach are that the amount of equipment in the field is greatly reduced. All signal processing would be confined to a central location, thereby simplifying maintenance, testing, and possible refinements and upgrades to the instrument. However, a careful evaluation of the potential effects of strong, narrow-band radiofrequency interference (RFI) and strongly variable signals of solar origin (flares) in gain compression will have to be performed.

#### 4.4. Data transmission

Optical fibers will be used to transmit data to and from the antennas. Optical fibers are inherently broad-band and are immune to RFI. The length of optical fiber runs in the FASR are modest. For an angular resolution of  $1''$  at 20 GHz, a maximum antenna baseline of 3 km is needed. The transmission losses will therefore be small. Optical fiber data transmission systems are currently in use at a number of existing or planned sites (e.g., the Australia Telescope and the Nobeyama Radioheliograph).

A disadvantage of optical fibers at present is the relatively low dynamic range imposed by optical-to-electrical and electrical-to-optical converters. The input signal is expected frequently to exceed that typical of quiet Sun conditions by 10 dB during flares. Exceptional events may elevate the input signal to 20, or even 30 dB, above quiet Sun levels. Some means of controlling the signal level is therefore necessary in the antenna front ends, irrespective of what type of analog signal processing is adopted. Optical fiber data transmission is used at the Nobeyama Radioheliograph; a single switched 10 dB attenuator was found to be sufficient to avoid dynamic range problems in the data transmission. The additional problem of exposure to RFI may be partially controlled through the use of notch filters at frequencies of the strongest and most persistent interference.

#### 4.5. Digital signal processing

At a central location the analog signals from the antennas will be further processed, including digitization, correction for delay, and, correlation. To avoid bandwidth smearing, the 500 MHz IF must be coarsely channelized into 16 or 32 spectral channels. The means by which this will be done has not been determined. One possibility is to channelize the analog data with a filter bank. Each analog channel can then be digitized, corrected for delay, and correlated in a continuum correlator. An alternative is to digitize the 500 MHz signal, correct it for delay, and then sent it to a lag correlator. The former places far fewer demands on the signal processing. The delay tolerances are modest and the sampling rates would be relatively low. It may be, however, that a hybrid solution involving both coarse channelization and a lag correlator will be optimum. If the entire RF spectrum is transmitted from the antennas to a central location, the details of signal processing may differ significantly.

Regardless of the details of its architecture, the correlator itself will likely perform one-bit, two-level sampling. The advantage of one-bit sampling is that it is immune to variations in the input signal levels, thus eliminating the need for tight control of the correlator inputs (as needed for two-bit, three- and four-level sampling, for example). One-bit correlation produces a correlation coefficient that must be multiplied by the system temperature to recover the correlated brightness on each baseline. Hence, a means of measuring the system temperature must be employed. One possible scheme is to monitor total power with a square-law detector and to monitor slow gain variations by injecting a broad-band calibration signal in the RF with a switching cycle compatible with the data sampling scheme adopted.

#### 4.6. Calibration

The need for a large FOV has led us to propose the use of 2 m antennas. Such small antennas will be insensitive to all sources on the sky except for the Sun. How will the complex gain of each antenna be calibrated? There are two possibilities: i) the antennas could be distributed so that all baselines were multiply redundant. A self-calibration scheme could then be employed such as that used at the Nobeyama Radioheliograph<sup>12</sup>; ii) one or more large, sensitive antennas could be used with the small antennas to calibrate the small antennas against sidereal sources of known position and flux density.

We prefer the latter option for several reasons. First, an instrument requirement is good absolute positional accuracy ( $< 1''$ ). A self-calibration scheme loses information about the absolute position of the source. Second, as we discuss in §4.1, the strawman antenna configuration provides desirable sampling and scaling characteristics that would be lost with a redundant spacing scheme. Finally, a redundant calibration scheme is a far less efficient use of a limited number of antennas – a nonredundant scheme extracts the most information about the visibility function. Instrument calibration on sidereal sources requires a small number of large, sensitive antennas. The construction of one or more new 25-m-class antennas would be prohibitively expensive. An affordable alternative is to refurbish existing antennas—e.g., one or both of the two 27 m antennas at Owens Valley, the three 25 m antennas at Green Bank, or one or more of the 25 m antennas at the VLA site. These will be used to calibrate the instrument against cosmic standards and could possibly also support high-resolution decimetric spectroscopy (see §4.8).

#### 4.7. Data processing and data products

As a fixed-configuration, solar-dedicated instrument, many of the data calibration, reduction, and archiving tasks can be automated. It is anticipated that the instrument will produce a large number of data products of great value to the research and space environment forecasting communities. These will be available rain or shine, and include:

1. Real-time precision flux spectra of the Sun as a star.
2. Near real-time data cubes that display the brightness temperature in two dimensions from chromospheric to coronal heights.
3. Near real-time coronal magnetograms that would provide the magnetic field strength at the base of the corona in active regions.
4. A real-time catalog of flares - their locations, morphology, and a number of indices characterizing their radio spectrum and its evolution.
5. A real-time list of prominence eruptions and CMEs.

Of course, many research projects will require complete and detailed analyses of the data. For example, flare studies will require deconvolved maps for every frequency and integration time. These reductions will be largely automated, but will likely be performed off line and then archived. Users will be able to access the archive in a flexible way. Sophisticated users may wish to work with raw data. The means will be provided to do so.

#### 4.8. Extensions and upgrades

While the core instrument will operate over a frequency range of 1-26.5 GHz, there are several obvious possibilities for extensions or upgrades to the core instrument. Since all are relatively stand-alone projects, any of them might lend itself to a foreign or domestic partner in the instrument.

One upgrade option is to extend the instrument to lower frequencies, perhaps as low as 300 MHz. This could perhaps be accomplished by means of a log-periodic crossed dipoles mounted at the vertex of the quadrupod of each antenna. The low-frequency feed would point outward, the antenna merely acting as a mount.

Another desirable upgrade is to extend frequency coverage to higher frequencies. Full support of millimeter bands could add considerable expense to the instrument. Cheaper alternatives are under consideration. One possibility is the use of a simple block converter to mix a broad-band portion of the high frequency spectrum down to a manageable frequency range.

A third upgrade option is to use the large antenna element(s) to perform high time- and spectral-resolution spectroscopy (non-imaging) at meter and decimeter wavelengths. Sensitive observations of classical radio bursts at meter wavelengths, flare-associated decimetric bursts (type III<sub>dm</sub> and type IV<sub>dm</sub> emissions), and broad-band spectral observations of noise storms, would enhance the scientific return of the FASR by coupling observational phenomena of the mid- to upper-corona with those of the low-corona and chromosphere probed by the microwave instrument.

### 5. SUMMARY

We have described a solar-dedicated instrument designed to integrate imaging and broad-band spectroscopic studies of the Sun: a frequency agile solar radiotelescope. The FASR will operate over core frequency range of 1-26.5 GHz, with possible extensions to lower (300 MHz) and higher frequencies (> 40 GHz). The FASR will be a fixed-configuration Fourier synthesis telescope. The optimum configuration will likely employ three or more linear arms of antennas, each 2 m in size. The antenna spacing will be distributed in a self-similar fashion to take advantage of frequency synthesis techniques, to obtain matched resolution at particular frequencies, and to sample the solar visibility function in an optimum way.

The data will be transmitted via optical fiber to a central processing point where the data will be digitized, correlated, calibrated, and archived for offline processing. The FASR will be calibrated against absolute flux standards of known position, enabling cross-comparisons with data from other wavelength regimes (e.g., X-ray and optical data) to a precision of order  $\lesssim 1''$ . Astronomical calibration will require the use of one or more large antenna elements ( $\sim 25$  m class) to calibrate the small elements.

The FASR will attack a broad range of scientific problems, from the ground, at modest cost. It will modernize radio studies of the Sun and allow multifrequency imaging on a par with the best available in other wavelength regimes. Radio diagnostics will be fully exploited for the first time to constrain coronal magnetic fields in both quiet and active phenomena, to study the acceleration and transport of energetic electrons, and to probe the structure of the quiet solar atmosphere. In addition, the FASR offers many data products of immediate and practical use to the space weather and geophysical forecasting communities, as well as inputs for the aeronomic and ionospheric studies. The instrument concept outlined above represents a distillation of many conversations and ideas from members of both the radio community and the broader solar community. These ideas were studied in some detail at an NSF and NASA supported Solar Radio Telescope Workshop, held in San Juan Capistrano, CA in 1995, and attended by about 40 US and international experts in solar radio physics. The FASR concept thus *represents a consensus opinion on the question of which direction ground-based solar radio astronomy can and must go in the near future.*

## REFERENCES

1. D. Gary and G. Hurford, "Coronal temperature, density, and magnetic field maps of a solar active region using the Owens Valley Solar Array," *Astrophys. J.* **420**, pp. 903–12, 1994.
2. T. Sakurai, K. Shibata, K. Ichimoto, S. Tsuneta, and L. Acton, "Flare-related relaxation of magnetic shear as observed with the Soft X-Ray telescope of Yohkoh with vector magnetographs," *Pub. Astro. Soc. Jap.* **44**, pp. L123–7, 1992.
3. T. Ayres and D. Rabin, "Observations of solar carbon monoxide with an imaging infrared spectrograph. I. thermal bifurcation revisited," *Astrophys. J.* **460**, pp. 1042–63, 1996.
4. H. Zirin, B. Baumert, and G. Hurford, "The microwave brightness temperature spectrum of the quiet sun," *Astrophys. J.* **370**, pp. 779–83, 1991.
5. M. Aschwanden, M. Montello, B. Dennis, and A. Benz, "Sequences of correlated hard x-ray and type iii bursts during solar flares," *Astrophys. J.* **440**, pp. 394–406, 1995.
6. T. Bastian and D. Gary, "On the feasibility of imaging coronal mass ejections at radio wavelengths," *J. Geophys. Res.* **102**, pp. 14031–40, 1997.
7. E. Schmahl and M. Kundu, "Synoptic radio observations," in *18th NSO/Sacramento Peak Workshop: Synoptic Solar Physics*, K. Balasubramaniam, J. Harvey, and D. Rabin, eds., ASP Conf. Ser., Brigham Young, Provo, 1997.
8. E. Keto, "The shapes of cross-correlation interferometers," *Astrophys. J.* **475**, pp. 843–52, 1997.
9. P. Napier, A. Thompson, and R. Ekers, "The Very Large Array: design and performance of a modern synthesis radio telescope," *IEEE* **71**, pp. 1295–1322, 1983.
10. T. Bastian, "Solar imaging with a synthesis telescope," in *Synthesis imaging in radio astronomy*, R. A. Perley, F. R. Schwab, and A. H. Bridle, eds., pp. 395–413, ASP Conf. Ser., Brigham Young, Provo, 1989.
11. R. Komm, G. Hurford, and D. Gary, "A spatial and spectral maximum entropy method as applied to ovro solar data," *Astron. Astrophys. Supp. Ser.* **122**, pp. 181–92, 1997.
12. H. Nakajima, S. Enome, K. Shibasaki, M. Nishio, and T. T. et al., "The Nobeyama Radioheliograph," *IEEE* **82**, pp. 705–13, 1994.